

1
2
3
4
5
6
7
8
9
10
11
12
13
14
15
16
17
18
19
20
21
22

Characterization of a Large Sexually Dimorphic Genome Interval in *Salix purpurea* L.
(Salicaceae)

Ran Zhou^{*}, David Macaya-Sanz^{*}, Eli Rodgers-Melnick^{*}, Craig H. Carlson[†], Fred E. Gouker[†],
Luke M. Evans^{*}, Jeremy Schmutz^{‡, **}, Jerry W. Jenkins[‡], Juying Yan^{**}, Gerald A. Tuskan^{**, ††},
Lawrence B. Smart[†], and Stephen P. DiFazio^{*}

^{*} Department of Biology, West Virginia University, Morgantown, WV 26506-6057
[†] Horticulture Section, School of Integrative Plant Science, Cornell University, New York State
Agricultural Experiment Station, Geneva, NY 14456
[‡] HudsonAlpha Institute of Biotechnology, 601 Genome Way Northwest, Huntsville, AL 35806
USA
^{**} Department of Energy Joint Genome Institute, 2800 Mitchell Drive, Walnut Creek, California
94598, USA
^{††} Biosciences Division, Oak Ridge National Lab

23
24
25
26
27
28
29
30
31
32
33
34
35
36
37
38
39
40
41
42
43
44
45
46

Running Title: Genomic Sex Dimorphism in *S. purpurea*

Key Words: sex, *Salix*, genome, suppressed recombination, dioecy

Corresponding Author:

Stephen P. DiFazio
Department of Biology
West Virginia University
53 Campus Drive
Morgantown, WV 26506-6057, USA
(304) 293-5314
spdifazio@mail.wvu.edu

47 **Abstract**

48 Dioecy has evolved numerous times in plants, but heteromorphic sex chromosomes are
49 apparently rare. Sex determination has been studied in multiple *Salix* and *Populus* (Salicaceae)
50 species, and *Populus* typically has an XY sex determination system on chromosome 19, while *S.*
51 *suchowensis* and *S. viminalis* have a ZW system on chromosome 15. Here we use quantitative
52 trait locus mapping and a genome-wide association study to demonstrate that *Salix purpurea* also
53 has a ZW system on chromosome 15. This region is characterized by reduced recombination,
54 high structural polymorphism, and an abundance of transposable elements, as expected for a sex
55 chromosome. Genes from this region are known to be involved in sex expression in other plants.
56 We also show that chromosome 19 has some sex chromosome characteristics in *S. purpurea*,
57 including significant QTL and association peaks for sex. Due to a lack of such signatures on
58 chromosome 15 in *Populus*, we hypothesize that sex determination was originally on
59 chromosome 19 in this lineage.

60 **Introduction**

61 Nearly 90% of flowering plants are hermaphroditic (containing both male and female floral
62 parts in the same flower), and less than 6% are dioecious (separate male and female individuals)
63 (Renner 2014). Evolutionary factors favoring dioecy include inbreeding avoidance and the
64 ability to maximize reproductive output through unisexual resource partitioning (Charlesworth
65 and Charlesworth 1978; Charnov 1982; Ashman 2006). In angiosperms, dioecy has
66 independently evolved hundreds of times from hermaphroditic progenitors (Renner 2014).
67 Evolutionary pathways to dioecy include gynodioecious, heterostylous, and monoecious
68 intermediates (Lloyd 1979; Ainsworth 2000; Charlesworth 2006), but monoecious intermediates
69 tend to be the most common mechanism in woody angiosperms (Olson *et al.* 2017).

70 Trait divergence between females and males can be facilitated by the presence of sex
71 chromosomes, as these are the only genomic regions that consistently differ between the sexes
72 (Rice 1984; Mank 2009; Barrett and Hough 2013). Sex chromosomes usually have suppressed
73 recombination and increased haplotype divergence due to independently accumulating
74 mutations, leading to the development of sexually dimorphic regions (SDR, regions that
75 consistently differ between males and females). The SDR may comprise a majority of the
76 chromosome or only a small portion. Heterogametic SDRs may confer either maleness (XY

77 system), as in *Silene latifolia*, *Carica papaya*, *Phoenix dactylifera*, *Diospyros lotus*, and *Populus*
78 *trichocarpa*; or femaleness (ZW system), as in *Fragaria chiloensis*, *Silene ottites*, and *Pistacia*
79 *vera* (reviewed in Charlesworth 2016; Vyskot & Hobza 2015). Sex chromosomes also contain
80 pseudoautosomal regions (PAR) where sex chromosomes recombine freely and may often show
81 elevated recombination (Nicolas *et al.* 2005; Otto *et al.* 2011). Many plant sex chromosomes are
82 homomorphic, exhibiting no strong morphological differences, suggesting that these
83 chromosomes are at an early stage of development (Ming and Moore 2007).

84 The Salicaceae family is an excellent model system for exploring the ecological and
85 evolutionary dimensions of dioecy and sexual selection in plants. Widely distributed across
86 temperate, boreal, and arctic regions of the globe, these genera represent a diverse assemblage of
87 catkin-bearing trees and shrubs (Karp *et al.* 2011). There are approximately 30 *Populus* species,
88 most of which are trees that grow in the northern hemisphere (Slavov and Zhelev 2010). In
89 contrast, there are approximately 500 *Salix* species, most of which are shrubs (Dickmann and
90 Kuzovkina 2014). Nearly all species in *Salix* and *Populus* are dioecious, but none have obvious
91 heteromorphic sex chromosomes (Peto 1938). *Salix* is primarily insect pollinated (Karrenberg *et al.*
92 *al.* 2002), and produces complex volatiles and nectar rewards (Füssel *et al.* 2007). In contrast,
93 *Populus* is almost exclusively wind-pollinated. Furthermore, both lineages share a well-
94 preserved whole genome duplication (Tuskan *et al.* 2006; Hou *et al.* 2016) and both show an
95 ongoing propensity toward polyploid formation (Mock *et al.* 2012; Serapiglia *et al.* 2015), thus
96 facilitating exploration of the relationship between polyploidy and sex chromosome evolution
97 (Ashman *et al.* 2013; Glick *et al.* 2016).

98 There has been considerable work on characterizing sex determination in *Populus* over the
99 past decade. The SDR has been mapped to the proximal telomeric end of chromosome 19 in *P.*
100 *deltoides* and *P. nigra* (Gaudet *et al.* 2008; Yin *et al.* 2008) and to a pericentromeric region of
101 chromosome 19 in *P. tremuloides*, *P. tremula*, and *P. alba* (Pakull *et al.* 2009; Paolucci *et al.*
102 2010; Kersten *et al.* 2014). In both *P. deltoides* and *P. alba*, the SDR was mapped on a female
103 genetic map but not on a male genetic map, possibly supporting female heterogamety (Yin *et al.*
104 2008; Paolucci *et al.* 2010). In *P. tremuloides* and *P. nigra*, the SDR was mapped on the male
105 genetic map and not on the female genetic map, suggesting male heterogamety (Gaudet *et al.*
106 2008; Kersten *et al.* 2014). Recently, a genome-wide association study (GWAS) on 52 *P.*
107 *trichocarpa* and 34 *P. balsamifera* found 650 SNPs significantly associated with sex. These sex-

108 associated markers were nearly fixed heterozygous in males and homozygous in females, which
109 is consistent with an XY sex-determination system (Geraldes *et al.* 2015). However, the
110 significant marker associations were not confined to chromosome 19 but were scattered
111 throughout the genome, possibly due to problems with assembly of the structurally-complex
112 SDR (Geraldes *et al.* 2015).

113 In contrast to *Populus*, the SDR has been mapped to chromosome 15 in *S. viminalis* and *S.*
114 *suchowensis* (Temmel *et al.* 2007; Hou *et al.* 2015; Pucholt *et al.* 2015). Furthermore, there is a
115 preponderance of female heterozygosity in the SDR of these species, indicating a ZW sex
116 determination system, in contrast to *Populus* (Hou *et al.* 2015; Pucholt *et al.* 2015). However,
117 neither study identified candidate genes in the *Salix* SDR that were orthologous to genes in the
118 SDR of *Populus* (Hou *et al.* 2015; Pucholt *et al.* 2015). Thus, *Salix* and *Populus* appear to have
119 different sex determination mechanisms or sex-determining genes, and the nature of the SDR in
120 the *Salicaceae* family remains poorly-characterized. In this study, we sought to explore the SDR
121 in an additional Salicaceae species, *Salix purpurea*. Using robust linkage and association
122 analyses, we show that the principal SDR is on chromosome 15, and that the genotype
123 configuration in this region is consistent with a ZW system of sex determination. Furthermore,
124 we also present evidence that chromosome 19 may retain a residual SDR that has been
125 superseded by the chromosome 15 locus.

126 **Materials and Methods**

127

128 **Genome Assembly**

129

130 This work is based primarily on v1.0 of the *S. purpurea* genome, which is being described
131 more completely in a separate publication (Smart *et al.*, in preparation). Briefly, a female diploid
132 genotype of *Salix purpurea* (clone 94006) was collected from the banks of the Fish Creek River
133 in Upstate New York in 1994 (43.2168 N, -75.6333 W). This clone has been an important parent
134 in *Salix* breeding programs, and is also the source of the reference genome that has been
135 developed by the Joint Genome Institute and a consortium of researchers (available at
136 <http://phytozome.jgi.doe.gov>). All DNA and RNA samples used for genomic and transcriptomic
137 sequencing were derived from clonally propagated individuals of this genotype. ALLPATHS-LG
138 was used to assemble sequences representing ~140X coverage of Illumina paired-end sequences,

139 as well as a set of mate-pair libraries (4.5 Kb, 5.3 Kb, 6.5 Kb), producing contigs with an
140 L50=46 kb and scaffolds with L50=191 kb. The ALLPATHS-LG assembly has a total length of
141 348 Mb and a total span of 392 Mb (including gaps) but is still relatively fragmented due to a
142 high level of heterozygosity (1 SNP per 120 bp, or 0.8%) and extensive structural variation.
143 Assessment of the assembly quality against willow BACs and transcripts suggested that ~ 78%
144 to 85% of the willow genome is captured in the current assembly. Gene annotations were
145 accomplished using the Phytozome pipeline (Goodstein *et al.* 2012). The RepeatModeler
146 (v1.0.8) package (<http://www.repeatmasker.org>) was used to identify and mask repetitive
147 elements.

148 **Genetic Mapping and Pseudomolecule Assembly**

149 An F₁ mapping population was produced by crossing two *S. purpurea* accessions, clone 94006
150 (female) and clone 94001 (male), and intercrossing two of the resulting progeny (female
151 ‘Wolcott’ and male ‘Fish Creek’) to produce over 500 F₂ progeny (referred to as Family 317).
152 The parents and progeny, were genotyped via “Genotyping by Sequencing” (GBS) using
153 *EcoT221* and *ApeKI* restriction enzymes, and 96-fold multiplexed sequencing on an Illumina
154 HiSeq Genome Analyzer (Elshire *et al.* 2011). SNPs were identified using the reference based
155 pipeline of TASSEL (Glaubitz *et al.* 2014) using the *S. purpurea* v1.0 reference genome
156 (available at <http://phytozome.jgi.doe.gov>). SNPs were also called using the UNEAK pipeline
157 from TASSEL (Glaubitz *et al.* 2014). SNPs were filtered using the following parameters: -
158 hetFreq 0.75 -mnTCov 0.01 -mnSCov 0.2 -mnMAF 0.05 -hLD -mnR2 0.2 -mnBonP 0.005, and
159 <40% missing data. A total of 8,531 informative GBS markers obtained from 411 F₂ progeny
160 were used to derive separate maps for markers in the three informative configurations: male
161 backcross (n=2623), female backcross (n=2211), and intercross (n=3697). These genetic maps
162 were integrated with the reference genome assembly to produce a combined map on which 276
163 Mb (70%) of sequence scaffolds were anchored, with intervening gaps that were proportional to
164 distances between mapped markers in the scaffolds. The remaining unplaced scaffolds contained
165 another 116 Mb of sequence. Assuming that the unplaced scaffolds are not alternative haplotypes
166 of the mapped scaffolds, the total estimated genome size is approximately 392 Mb, an estimate
167 that was corroborated by kmer counting and flow cytometry (Smart *et al.*, in preparation). The
168 assembly was compared to the *Populus trichocarpa* v3.0 reference genome with LASTZ
169 (v1.03.66), using parameters to exclude alignments between paralogous segments derived from

170 the most recent shared whole genome duplication (gapped, chain, transition, maxwordcount=4,
171 exact=100, step=20).

172 **Identification of Sexually Dimorphic Genome Regions**

173 Sex was scored for F₂ progeny by repeated observations during the spring of 2012, 2013,
174 and 2015 in common gardens at the New York State Agricultural Experiment Station (Cornell
175 University) in Geneva, NY. Quantitative Trait Locus (QTL) mapping was performed using the
176 r/QTL package in R with a binary phenotype model (Arends *et al.* 2010). Logarithm of odds
177 (LOD) support intervals or an approximate Bayesian credible interval were calculated using
178 r/QTL. QTL mapping was performed for all three genetic maps (female backcross, male
179 backcross and intercross).

180 We also performed a Genome-Wide Association Study (GWAS) on the sex trait using a
181 population of unrelated individuals collected from the wild. A population of 112 *Salix purpurea*
182 individuals was collected from upstate New York, Pennsylvania, Connecticut, and Vermont and
183 planted in common gardens at Cornell University in Geneva, NY and at West Virginia
184 University in Morgantown, WV. Sex was scored in the spring of 2013 and 2014 for six clonal
185 replicates at each site. Only individuals for which sex was consistently and unambiguously
186 scored as male or female were used for the analysis. The population was genotyped using GBS
187 with the *ApeKI* restriction enzyme and 48-fold multiplex sequencing on an Illumina HiSeq
188 Genome Analyzer. SNPs were called and filtered as described above, yielding 85,543 SNPs for
189 analysis. A kinship matrix was calculated using the scaled Identity-by-State (IBS) method
190 implemented in the EMMAX package (Kang *et al.* 2010). Clonal ramets were identified based
191 on pairwise IBS values in comparison to pairwise IBS of the F₂ population described above
192 (Figure S1). This resulted in removal of 34 ramets belonging to 9 clonal groups. Three
193 apparently hermaphroditic individuals and 12 individuals with inconsistent sex phenotypes were
194 also excluded from this analysis, leaving a total of 38 females and 22 males. To control for the
195 influence of population structure, a Principal Components Analysis (PCA) was performed using
196 smartPCA in the Eigenstrat package (Price *et al.* 2006). GWAS for sex was performed with the
197 first two principal components and the kinship matrix as covariates using a mixed linear model
198 implemented in the EMMAX package (Kang *et al.* 2010). We controlled for multiple testing
199 using a Bonferroni correction with an alpha value of 0.05.

200

201 **Characterization of the Genomic Composition of the SDR**

202 We defined the SDR intervals based on all GWAS loci that passed the Bonferroni
203 correction. SDR intervals were initially defined as +/- 5 kb around each significant GWAS locus.
204 Also, because the SDR region is structurally complex and repetitive, the genome assembly is
205 likely to be inaccurate in this region, thereby reducing the resolution of the GWAS and QTL
206 mapping. We therefore merged all SDR intervals that occurred within 1 Mb on the same
207 chromosome to include all intervening sequence.

208 To identify levels of polymorphism and divergence between the consensus reference and
209 female-specific haplotypes, we resequenced the F₁ female parent 94006 and the F₂ male parent
210 ‘Fish Creek’ using 2×250 bp reads on an Illumina HiSeq sequencer. This yielded 106,305,281
211 paired reads (53 Gb) and 92,077,639 paired reads (46 Gb), respectively. These were aligned to
212 the 94006 reference genome using Bowtie2 with the parameters -D 15 -R 2 -N 0 -L 20 -i
213 S,1,0.75. SNPs were identified using the mpileup function of samtools, followed by bcftools with
214 the parameters -g 1 -O v -m. Since ALLPATHS-LG generates genome assemblies that consist of
215 chimeras of the two haplotypes from a heterozygous diploid genome (Gnerre *et al.* 2011), we
216 expected the *S. purpurea* assembly of chromosome 15 to include segments of Z and W
217 chromosomes. This should be apparent from the relative depth of coverage of female and male
218 sequences. For Z portions of the reference genome, male coverage should be roughly double that
219 of the female for divergent portions of the SDR, whereas for W portions of the reference,
220 coverage should be approximately 0.5X compared to the rest of the genome for the female, and
221 there should be zero coverage in males. We therefore used these alignments to evaluate depth of
222 coverage for the male and female sequences using raw output from the samtools mpileup
223 command to delineate putative Z and W portions of the reference. Similar expectations hold for
224 the GBS markers, which should be homozygous in females and null in males when mapped to
225 the divergent W portions of the reference genome.

226 We identified female-specific alleles for loci that were heterozygous in the female parent
227 clone 94006 and homozygous in the male offspring, Fish Creek. Sequences containing female-
228 specific polymorphisms (here called “W-type”) were created using the
229 FastaAlternateReferenceMaker module of the GATK package (DePristo *et al.* 2011). For
230 comparison, we also used all polymorphisms from the resequencing of both genotypes to create
231 alternative haplotypes using the same approach. Genes with nonsense and frameshift mutations

232 were then removed as possible pseudogenes. Finally, synonymous (dS) substitution frequencies
233 were estimated for all pairs of predicted transcripts using the ‘*yn00*’ module in the PAML
234 package (Yang 2007). The reference genome transcripts were compared to those containing
235 female-specific polymorphisms as well as to those containing all alternative alleles.

236 All predicted proteins in the *S. purpurea* reference genome annotation were compared to
237 the UniProt database (<http://www.uniprot.org/>) using blastp and against the Pfam database
238 (<http://pfam.xfam.org/>) using HMMER, with default parameters. Protein mapping results were
239 submitted to Argot² (Falda *et al.* 2012) to obtain Gene Ontology (GO) annotations, using a
240 stringent cut-off (Total Score=1500) to filter Type I errors. We used Fisher’s Exact Test to
241 identify overrepresented GO terms for candidate genes in the SDR. All orthologs between *S.*
242 *purpurea* and *P. trichocarpa* were retrieved from Phytozome (<https://phytozome.jgi.doe.gov/>).
243 Synonymous (dS) and nonsynonymous (dN) substitution frequencies were estimated for each
244 pair of primary transcripts from each species using the ‘*yn00*’ module in the PAML package
245 (Yang 2007). Pairs with dS>0.4 were dropped, assuming they were incorrectly defined as
246 orthologs. In total, 33,789 ortholog pairs were compared, including 27,118 genes from *S.*
247 *purpurea* and 24,000 genes from *P. trichocarpa*.

248 **Estimation of Recombination Rate**

249 As an indicator of recombination rate, we calculated the ratio of physical to genetic
250 distance between marker pairs using linkage groups with >30 markers. For each linkage group,
251 pairwise distances were calculated between every N loci, where N was 10% of the total number
252 of loci on the linkage group. For example, if the linkage group had 100 markers, the distance was
253 calculated between all pairs of loci that were separated by 10 loci. Negative and extreme values
254 (ratio>15) were removed for the purpose of visualization.

255 **Gene Expression**

256 RNA sequencing was performed for actively growing shoot tips for five male and five
257 female progeny from the family used for QTL analysis. Detailed methods are described in
258 Carlson *et al.* (2017). Briefly, total RNA was extracted using the SpectrumTM Total Plant RNA
259 Kit. Libraries were constructed using the NEBNext Ultra Directional RNA Library Prep Kit.
260 Libraries were sequenced on the Illumina HiSeq platform (1x100 bp) yielding an average of 17.9
261 million mapped reads per sample. Reads were mapped to the *S. purpurea* reference genome v1.0

262 using the CLC Genomics Workbench, and differential expression analyses were performed using
263 EdgeR.

264 Results

265 266 Localization of the SDR to Chromosome 15 and Chromosome 19

267 Among the 396 phenotyped and genotyped individuals in the F₂ family, there were 234
268 females and 162 males. This ratio is significantly skewed toward females (F:M=1.44; $\chi^2=13.1$;
269 df=1; $P<0.001$). QTL mapping identified sex-associated markers principally on chromosome 15
270 for all three maps (Figure 1; Table S1). On the female map, 125 markers were linked to sex, 105
271 of which were on chromosome 15, spanning from 225.42 cM to 240.17 cM (Table 1). On the
272 male map, only five markers were linked to sex, four of which were in the interval from 326.48
273 cM to 347.17 cM on chromosome 15 (Figure 1, Table 1). An additional 50 markers were linked
274 to sex on the intercross map, covering an interval of about 2.6 cM, all on chromosome 15 (Figure
275 1, Table 1). Based on anchoring mapped markers to physical positions in the *S. purpurea*
276 genome assembly, the potential SDR can be mapped to two regions on chromosome 15 ranging
277 from ~0.4 Mbp to 1.9 Mbp and from ~10.9 Mbp to ~15.1 Mbp.

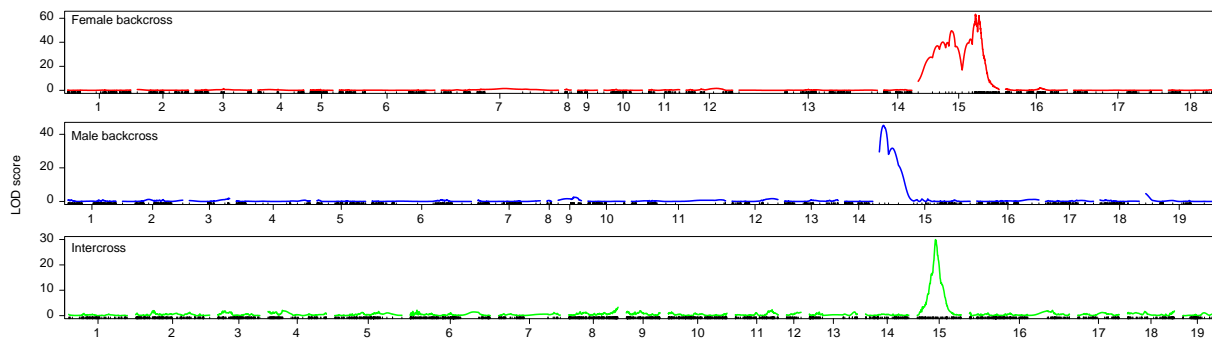


Figure 1 QTL for sex in an F₂ *S. purpurea* cross. From top to bottom are LOD scans for female backcross (red), male backcross (blue) and intercross (green) markers across the 19 major *S. purpurea* linkage groups. Chromosome 15 has a very strong QTL sex in all three maps, and the female backcross also shows a weak peak on chromosome 19 (LOD=4.68; table 1).

278

279 **Table 1** Bayesian credible intervals for sex QTL on chromosome 15.
 280

	Physical Map		Genetic Map	
	Start (bp)	End (bp)	Start (cM)	End (cM)
Female Map	10,939,613	11,569,298	225.42	240.17
Male Map	372,445	1,881,243	326.48	347.17
Intercross	11,401,384	15,091,498	55.69	58.22

281
 282 One additional sex-linked marker was located at the proximal end of chromosome 19 on
 283 the male map, with a LOD score of 4.68 (Figure 1; Table S1). However, mapping failed entirely
 284 for chromosome 19 for female backcross markers, the only chromosome for which this was the
 285 case. Chromosome 19 had the lowest density of GBS markers in the genome (Table S2).
 286 Furthermore, this chromosome had the lowest proportion of markers in a female-backcross
 287 configuration, and the highest proportion of markers with severe segregation distortion (Figure
 288 S2; Table S2).

289 To confirm the location of the SDR in a diverse population, a GWAS for sex was
 290 performed using naturalized *S. purpurea* accessions collected from northeastern North America.
 291 Of the 60 genets that were unambiguously phenotyped for sex, 38 were female and 22 were
 292 male, which is a significantly female-biased sex ratio (F:M=1.73; $\chi^2=4.3$; df=1; $P=0.02$). Of the
 293 85,543 SNP markers that passed filtering, 72 were significantly associated with sex ($P<5.85 \times$
 294 10^{-7} , Figure 2; Figure S3). Among these markers, 41 were located on chromosome 15, from 10.7
 295 Mb to 15.3 Mb, and four were located at the distal portion of chromosome 15 (1.9 Mbp). Thus,
 296 the primary SDR identified by GWAS overlaps with those mapped by QTL in the F₂ family
 297 (Figure 3). In addition, six markers from chromosome 19 at ~69 kb were also significantly
 298 associated with sex (Figure 2), which also corresponds with the QTL results. Additionally, there
 299 were minor peaks on chromosomes 1,2,3, and 5, and there were six scaffolds containing a total
 300 of 13 significant sex-associated markers that were not anchored to the genetic maps (Table S3).

301 To evaluate whether these secondary chromosomal peaks could have been due to
 302 assembly errors, we aligned these SDR sequences to the *S. purpurea* reference genome using
 303 blastn. None of these chromosomal loci shared homology with the chromosome 15 SDR (Table
 304 S4). We also compared these SDR sequences to the *Populus trichocarpa* v3.0 reference genome
 305 using blastn. The SDRs on chromosomes 1,2, and 5 had best hits to the same chromosomes in *P.*
 306 *trichocarpa*. However, the SDRs on chromosomes 3 and 19 had best hits to scaffold_25 in *P.*

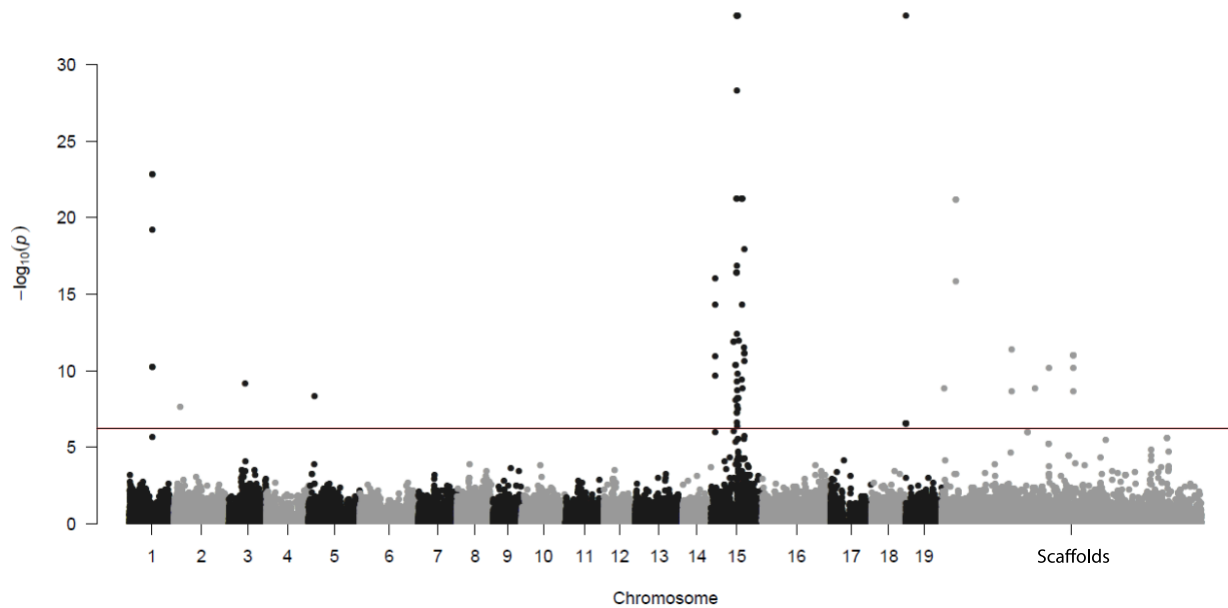


Figure 2 Manhattan plot derived from genome-wide association analysis for sex determination. The Y-axis shows the strength of association ($-\log_{10}(P$ value)) for each SNP ordered by chromosome and SNP position (x axis). The horizontal line indicates significance after a Bonferroni correction for multiple testing.

307 *trichocarpa* (Table S4). Because the SDR is known to be poorly assembled in the *P. trichocarpa*
 308 v3.0 assembly (Geraldes *et al.* 2015), we aligned scaffold_25 to the *P. trichocarpa* v1.0
 309 assembly and found that it matched primarily to chromosome 19, positions 751 to 1040 kb,
 310 which coincides with the main *P. trichocarpa* SDR (Geraldes *et al.* 2015). Therefore, the QTL
 311 and GWAS results both indicate that sequences homologous to the *P. trichocarpa* SDR retain
 312 evidence of sex dimorphism in *S. purpurea*.

313 ***S. purpurea* Has a ZW System of Sex Determination**

314 Under Mendelian segregation, the frequency of heterozygotes should be 0.5 for both male
 315 and female F_2 progeny. However, the frequency of heterozygosity was 0.64 for female progeny
 316 and only 0.12 for males (Table S1). The skewed heterozygosity occurred in blocks in the vicinity
 317 of the sex QTL peaks (Figure 3). Furthermore, females in the association population had an
 318 average observed heterozygosity of 0.79 for the sex-associated SNP loci, while males had an
 319 observed heterozygosity of only 0.05 for these same loci (Figure 4a, Table S3, Figure S4). This
 320 difference was significant based on a t-test ($P < 2.2 \times 10^{-16}$). Both observations are consistent with
 321 a female heterogametic (ZW) system of sex determination, where females should be nearly fixed
 322 heterozygous for female-specific portions of the SDR, while males should be homozygous for

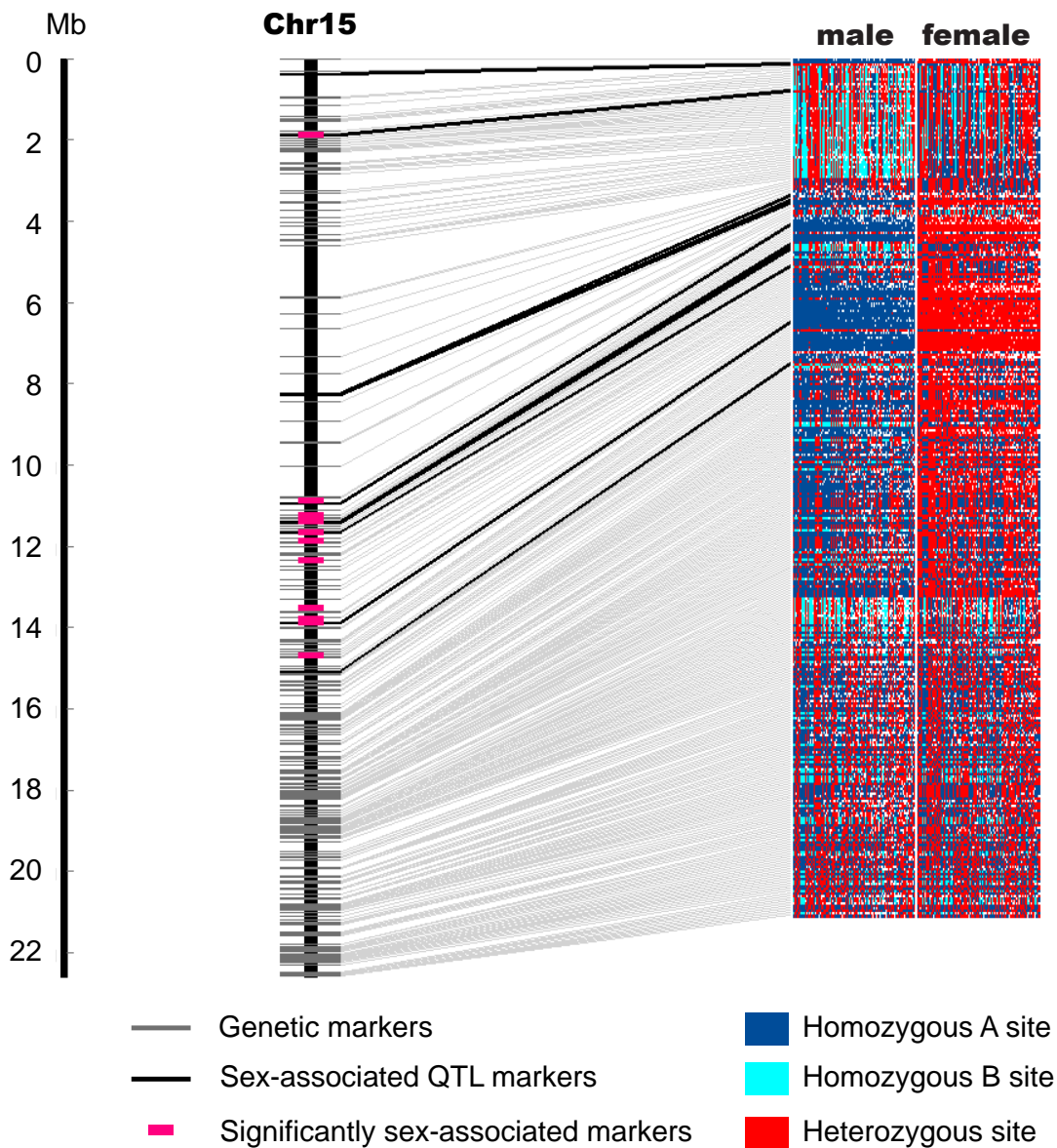


Figure 3 Genotype configurations in males and females from the F₂ family on chromosome 15. Markers from all three genetic maps are shown as horizontal lines corresponding to their physical positions on the chromosome 15 physical assembly. Markers with top LOD scores in each map are colored as black. Significantly associated markers from the GWAS analysis with $P < 1 \times 10^{-7}$ are indicated by fuschia marks on the physical map. Each marker is connected between physical map and its genotype configurations with 100 selected progeny of each sex. Genotypes of QTL markers are colored according to their homozygosity or heterozygosity.

324 those same loci. This is due to the typically biallelic nature of SNP polymorphisms, where
325 polymorphic alleles from the W chromosome are identical by descent and therefore only occur in
326 females. The discrepancy between the observed values and the expected fixed heterozygosity in
327 females is likely due to null alleles caused by allele dropout and/or inadequate sequencing depth
328 for the GBS markers (Andrews *et al.* 2016).

329 Since our reference sequence was derived from a female, we expected that the assembly
330 could contain hemizygous or highly divergent portions of the W chromosome. We used two
331 complementary approaches to determine the size and extent of these regions: allelic
332 configurations of the GBS markers, and relative depth of sequence coverage in male and female
333 clones. Candidate W segments contained a large proportion of GBS markers that were
334 homozygous in females and mostly lacking genotype calls (i.e., double null markers) in males in
335 the association population (Figure S5). We identified 231 of these W-type markers (0.27%)
336 (Figure 4a; Table S5). Of these, 51 occurred on chromosome 15, another 158 occurred on 20
337 unanchored scaffolds, and the remaining 22 occurred on small segments of chromosomes 3, 5,
338 and 7. The genotype configuration for these markers was consistent with a ZW system, such that
339 the average observed homozygosity for females was 0.80 (presumably due to hemizyosity or
340 divergence of W segments) whereas 85% of males had null alleles at these loci, on average
341 (Figure 4a, Table S5). The putative W haplotypes were interspersed along chromosome 15,
342 suggesting that the genome assembly is a chimeric representation of the Z and W haplotypes
343 (Figure 4a; Table S5).

344 We also examined depth of coverage in male and female reference-based assemblies to
345 identify putative hemizygous W chromosome segments in the reference genome. If females are
346 heterogametic, then there should be regions in the female reference that are not covered by reads
347 from a male individual. Aligning paired 250 bp Illumina sequences from a male offspring ('Fish
348 Creek') of clone 94006 back to the female reference assembly, yielded a very high alignment
349 rate of 95.19% compared to 96.67% when clone 94006 was aligned to itself. Nevertheless, after
350 excluding known repeats and gaps, there were 22,733 regions totaling 7.69 Mb on chromosomes
351 and another 6.87 Mb of unanchored scaffolds that had coverage in the female but lacked
352 coverage in the male (Table 2; Figure S6). These analyses identified 222 scaffolds comprised of
353 >30% female-specific sequences (Table S5). Some of these are likely caused by
354 insertion/deletion polymorphisms that are not sex-specific. However, we identified 11 scaffolds

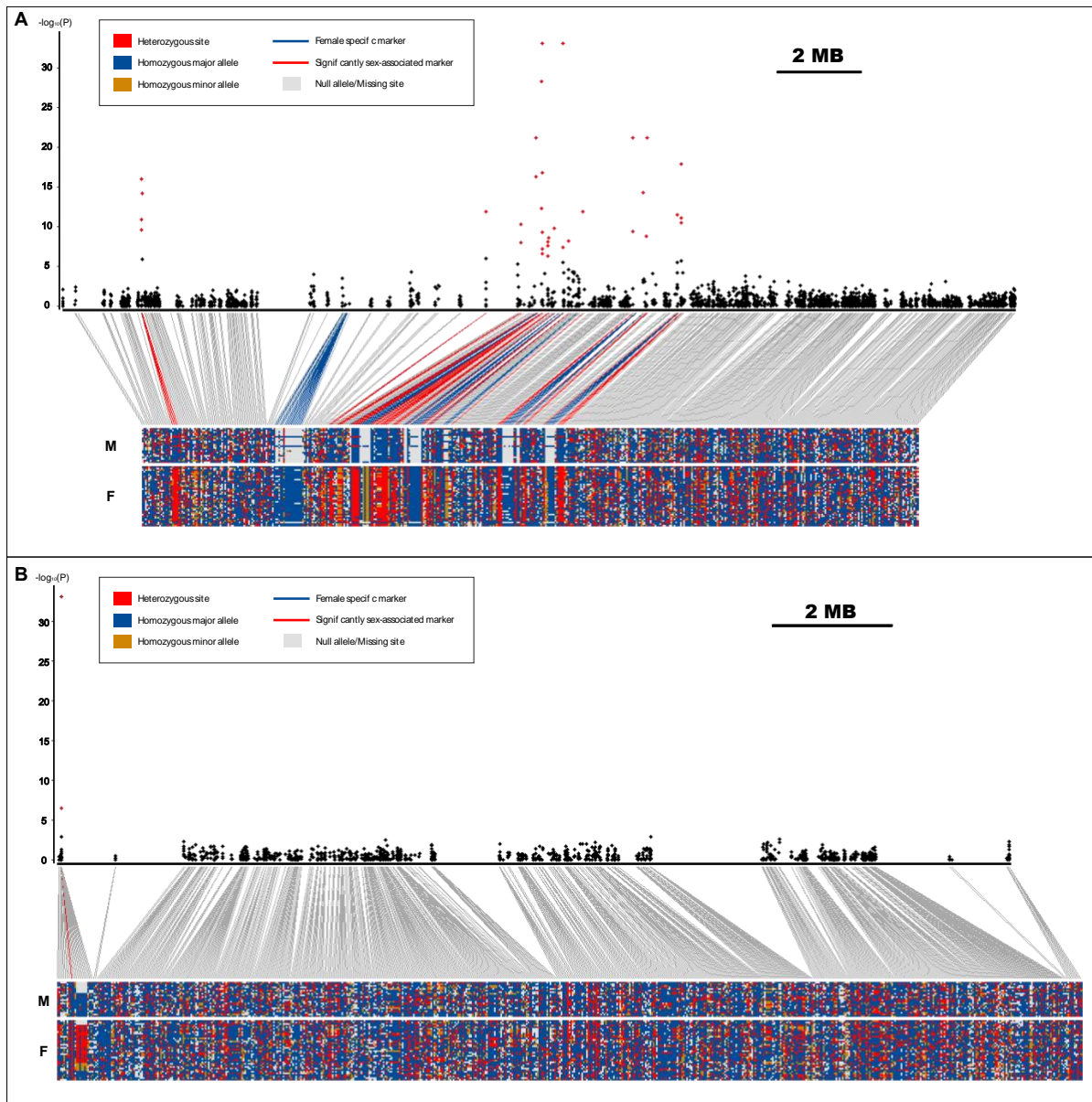


Figure 4 Genotype configurations of markers on chromosome 15 (A) and chromosome 19 (B) from the *S. purpurea* association population. The top is a blowup of chromosome 15 from the Manhattan plot in Figure 2, with significantly sex-associated markers colored red. The bottom shows the genotype configurations of 22 males and 38 females from the association population, where each row represents an individual. “Major alleles” are here defined as those with higher frequency in males, and are shaded blue where homozygous, while homozygotes for male minor alleles are shaded gold. Heterozygous sites are shaded red, and missing data is light gray. Lines connect each plotted marker to its physical position. Red lines indicate that markers are significantly associated with sex while blue lines indicate the markers were identified as female-specific (putatively derived from the W haplotype).

356 that were also identified as putative W segments based on allelic configurations (see above).
 357 Portions of five of these scaffolds had high sequence similarity to chromosome 15, supporting
 358 the contention that these are alternate haplotypes from the SDR. For example, Scaffold0265 is
 359 298 kb in length and contains 38.9% female-specific sequence and 20 W-type GBS markers
 360 (Table S6). This scaffold also contains three sex-associated markers identified in the GWAS.
 361 Cumulatively, these 11 scaffolds covered 1.04 Mb, which is a reasonable lower limit for the size
 362 of the divergent portions of the SDR.

363

364 **Table 2** Length of intervals that lacked coverage in alignments of 2x250 bp reads against the
 365 reference genome assembly (also derived from female clone 94006). Number in the parentheses
 366 is the percentage of the total genome composition in that category that lacked coverage.

367

	Whole Genome	Fish Creek (♂)	94006 (♀)
Total Length	348,745,509	14,564,089 (4.18)	562,813 (0.16)
Chromosomes	251,661,964	7,693,428 (3.06)	303,356 (0.12)
Scaffolds	97,083,545	6,870,661 (7.08)	259,457 (0.27)
Repeats	98,506,863	5,328,429 (5.41)	260,598 (0.26)
Genes	120,852,638	2,654,305 (2.20)	78,325 (0.06)
SDR	3,073,122	480,360 (15.63)	4,814 (0.16)

368

369

370 **The SDR is Highly Repetitive, Has Repressed Recombination, and is Divergent from the**
 371 ***Populus* SDR**

372 The SDR on chromosome 15 of *S. purpurea* overlaps with a large region (9.8 Mb to 16.2
 373 Mb) with elevated physical-to-genetic distance ratio of 0.867 Mb/cM, compared to the genome-
 374 wide average of 0.172 Mb/cM (Figure 5), which indicates reduced recombination. This interval
 375 contained high repeat abundance relative to the rest of the genome (Figure S7). A portion of the
 376 SDR in *S. purpurea* is homologous to the SDR in *S. suchowensis*. The *S. suchowensis* SDR
 377 primarily occurs on scaffold64, an ~900 kb scaffold that maps to chromosome 15 (Hou *et al.*
 378 2015). Aligning this sequence to the *S. purpurea* genome with lastz, we observed homology
 379 from 6.2 to 7.3 Mb and from 14.1 and 15.1 Mb on *S. purpurea* chromosome 15 (Figure S8). The
 380 latter sequence overlaps with a portion of the *S. purpurea* SDR. In contrast, the *S. viminalis* SDR

381 matches from 5.9 to 8.4 Mb on *S. purpurea* chromosome 15, which is outside the *S. purpurea*
382 SDR (Pucholt, Wright, *et al.* 2017).
383

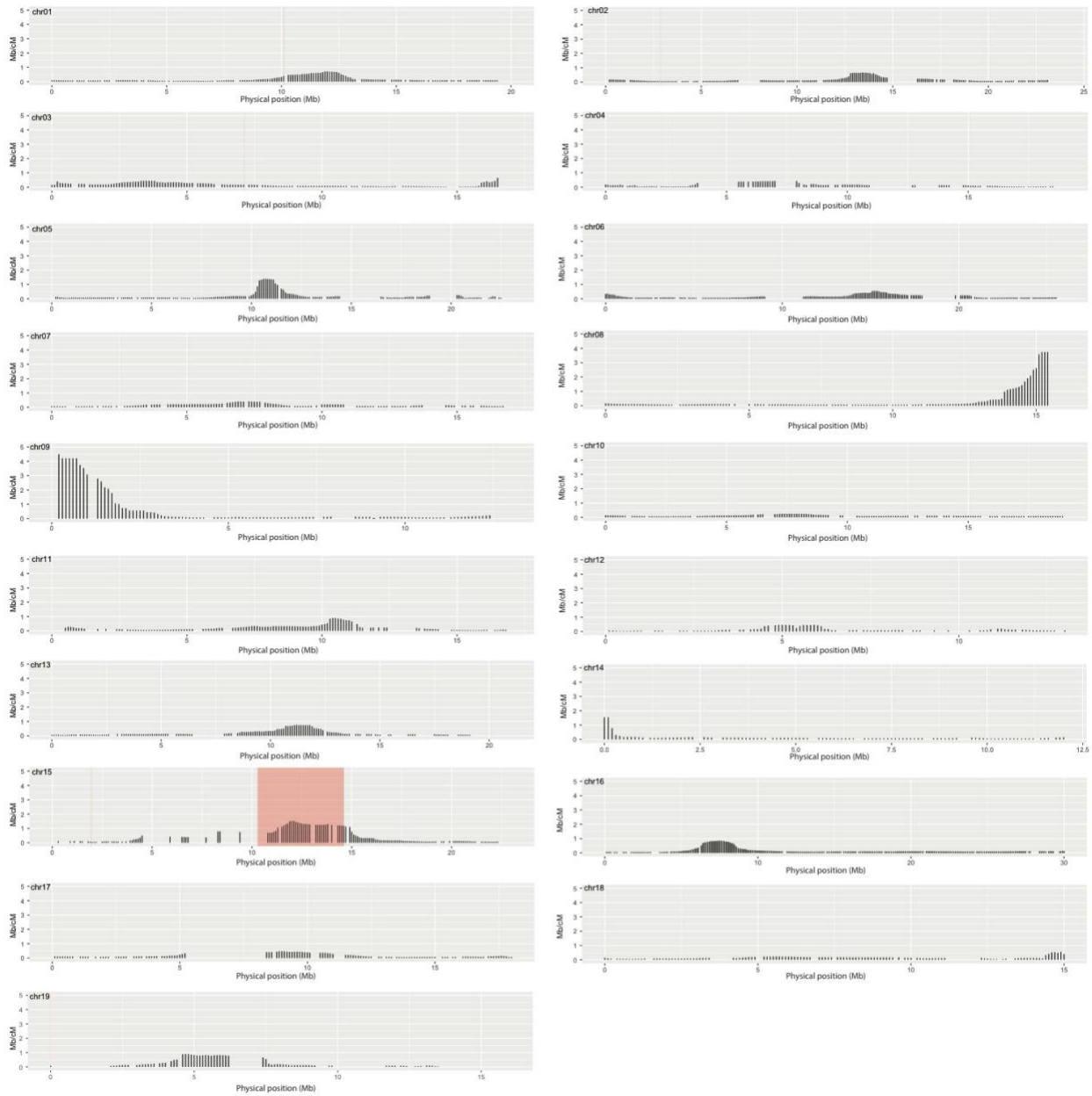


Figure 5 Recombination across the *S. purpurea* genome, as inferred from physical:genetic distance ratio. Bar plots represent the physical:genetic distance ratio (Mb/cM) in 100 kb windows for the 19 chromosomes. The position of the SDRs are indicated by vertical red shading.

384 *P. trichocarpa* is another member of the Salicaceae and has a fairly-well characterized
 385 XY system of sex determination (Gerald *et al.* 2015). In general, *S. purpurea* and *P.*
 386 *trichocarpa* have high synteny at the chromosome scale (Figure 6), but chromosome 15 in *S.*
 387 *purpurea* stands out in several ways. First, the SDR on chromosome 15 of *S. purpurea* is not
 388 syntenic with chromosome 15 or any other chromosome of *P. trichocarpa* (Figure 6). Second,
 389 the proportion of repeats is significantly elevated in the *S. purpurea* SDR, with an average of
 390 37% repeat composition, compared to the genome-wide average of 24.8% (Welch's Two-Sample
 391 T = -4.6 P5948, <0.0001; Table S7; Figure S7). Chromosome 19, which contains the SDR in *P.*
 392 *trichocarpa*, also had the highest average repeat content in *S. purpurea* (33.5%, compared to
 393 25.1% genome-wide average) (Table S7).

394 **Gene Content of the SDR**

395 We identified 251 protein-coding genes within the *S. purpurea* SDR (Table S8). A GO
 396 enrichment analysis based on 203 genes annotated with GO terms identified 4 significantly
 397 enriched terms (Bonferroni adjusted $P < 2.45 \times 10^{-4}$), all of which were related to microtubule
 398 functions. These include microtubule-based movement (GO:0007018), microtubule motor
 399 activity (GO:0003777) and microtubule binding (GO:0008017), as well as kinesin complex
 400 (GO:0005871) (Table 3). This enrichment is partly due to two pairs of tandemly-duplicated
 401 kinesin-like genes in the SDR (Table S8). Since there is only one homolog of these kinesin-like
 402 genes in *P. trichocarpa*, it appears that this expansion occurred after the divergence of the two
 403 genera, a scenario supported by high sequence conservation between the tandem duplicates
 404 (Figure S9).

405

406 **Table 3** Significantly overrepresented GO terms of candidate genes from SDR.

407

Description	GO term	Number of genes in SDR	Number of genes outside SDR	P value
Microtubule motor activity	GO:0003777	7	91	4.73 x 10 ⁻⁶
Kinesin complex	GO:0005871	7	92	5.07 x 10 ⁻⁶
Microtubule-based movement	GO:0007018	7	92	5.07 x 10 ⁻⁶
Microtubule binding	GO:0008017	7	133	4.84 x 10 ⁻⁵

408

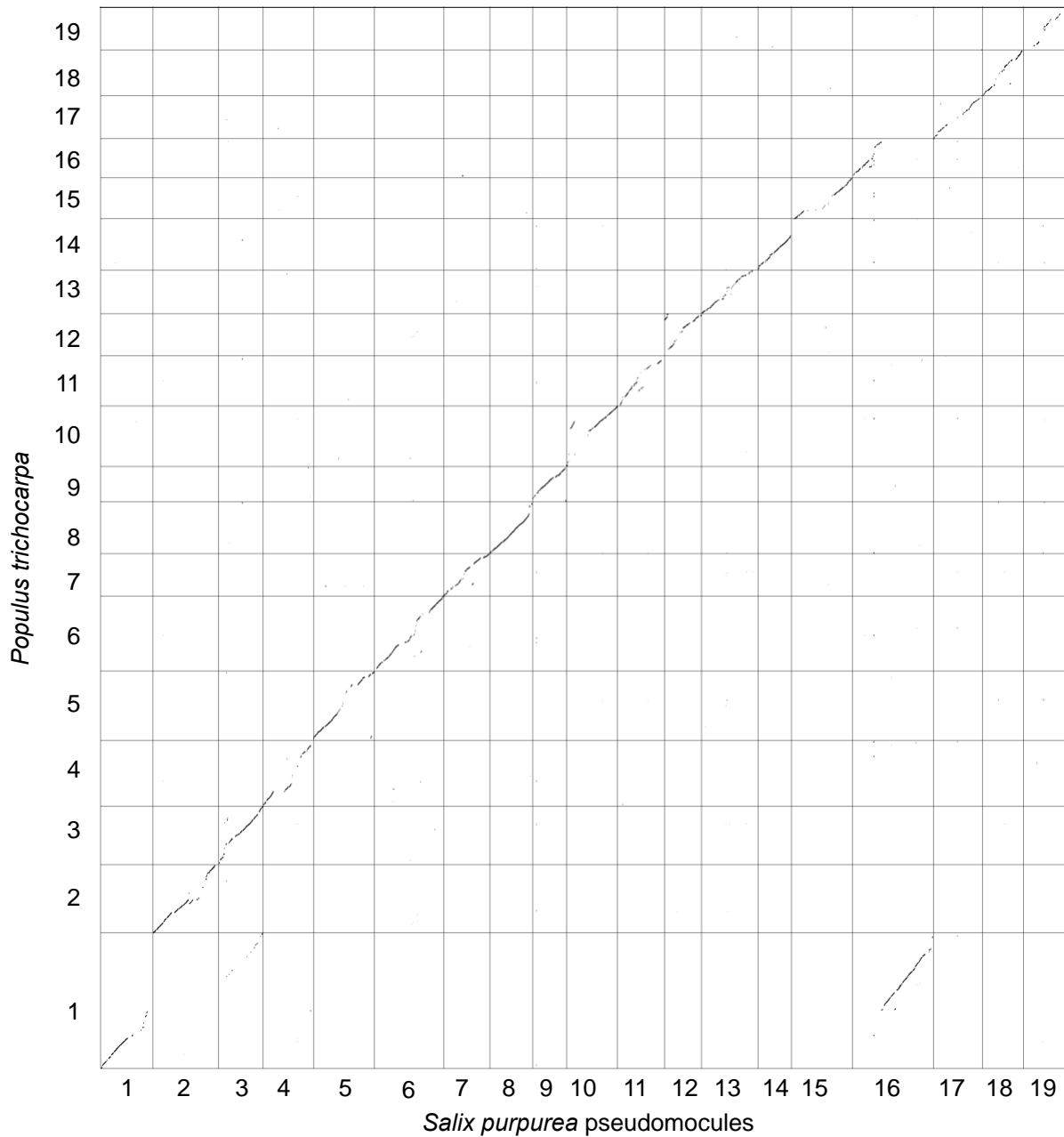


Figure 6 Comparison between the *S. purpurea* (x-axis) and *P. trichocarpa* (y-axis) genomes. The two genomes are largely syntenic based on genome-scale alignments using LASTZ, with parameters set to exclude paralogous segments derived from the most recent whole genome duplication.

410 The SDR contains 20 genes that have >70% female-specific sequence, and many of these
411 genes also show sex-biased expression in stem tissue in *S. purpurea* (Table S8; Carlson *et al.*
412 2017). These include an extracellular calcium-sensing receptor (SapurV1A.0301s0080), an auxin
413 response factor (SapurV1A.0718s0100), a peptidase M50B-like protein (SapurV1A.0475s0170),
414 a zinc finger C3hC4 type transcription factor (SapurV1A.0301s0170), and a reticulon-like
415 protein (SapurV1A.0530s0130). Among these, only the reticulon-like protein showed an
416 elevated dN/dS ratio when compared to *P. trichocarpa* (0.687, versus a genome-wide average of
417 0.406). Of the 14 genes that showed significant female-biased expression in the SDR, only one
418 lacked female-specific sequence (SapurV1A.1386s0030, a small heat shock protein). No genes
419 showed significant male-biased expression after Bonferroni correction.

420 The chromosome 19 SDR is of particular interest, since it overlaps with the SDR of *P.*
421 *trichocarpa*. This region spans approximately 10 kb in the current assembly, and harbors three
422 small genes. SapurV1A.1005s0060 contains a Small MutS-Related (SMR) domain. A second
423 gene, SapurV1A.1005s0050, is a calcium-dependent kinase with two EF-Hand domains. The
424 third gene, SapurV1A.1005s0070, encodes a hypothetical protein (Table S8). None of these
425 genes have sex-biased expression or unusual dN/dS ratios compared to *Populus* (Table S8).

426 We attempted to estimate the relative age of the region of suppressed recombination by
427 estimating the rate of synonymous substitution of W alleles compared to Z alleles in the SDR.
428 Calculated this way, the Z-W synonymous substitution rate within the SDR was 0.00343 while
429 the rate calculated the same way outside of the SDR was 0.00151. These differences were
430 statistically significant ($t = -4.099$; $df = 249$; $P = 5.63e-05$). For comparison, we also calculated
431 divergence between alleles using all observed polymorphisms. Genes within the SDRs showed
432 similar overall divergence (dS=0.00616) compared to genes outside the SDRs (dS=0.00607), and
433 the difference was not significant ($t = -0.077$; $df = 235$; $P = 0.938$). There was no evidence of
434 evolutionary strata in the SDR based on lack of clustering of genes with similar dS values.

435 Discussion

436 437 **The *S. purpurea* SDR is Similar to Other *Salix* Species and Divergent from *Populus***

438
439 In all three of the *Salix* species studied thus far, *S. viminalis* (Pucholt *et al.* 2015), *S.*
440 *suchowensis* (Hou *et al.* 2015; Chen *et al.* 2016), and now *S. purpurea*, the largest SDR is on

441 chromosome 15, and shows clear female heterogamety. Furthermore, the *S. suchowensis* SDR
442 overlaps with a portion of the *S. purpurea* SDR, but the *S. viminalis* SDR does not. This may
443 reflect the evolutionary distinctness of *S. viminalis* from the other two taxa. Based on
444 morphological characters, *S. viminalis* belongs to section *Viminella*, which is strongly
445 differentiated from section *Helix*, which contains *S. purpurea* (Argus 1997). This is similar to the
446 situation in *Populus*, where the location of the sex determination region varies across different
447 sections of the genus, though all are located on chromosome 19 (Gaudet *et al.* 2008; Pakull *et al.*
448 2009, 2014; Paolucci *et al.* 2010; Tuskan *et al.* 2012; Kersten *et al.* 2014; Geraldès *et al.* 2015).
449 Comparison of the sequence composition of the *Salix* SDRs and the *P. trichocarpa* SDR
450 revealed no extensive stretches of homology, suggesting a largely independent evolution of these
451 genome regions (Hou *et al.* 2015; Pucholt, Hallingbäck, *et al.* 2017). Clearly, the SDR is highly
452 dynamic within this family.

453 The alternative peaks from the GWAS analysis on chromosomes 1, 2, 3, and 5 were not
454 upheld by the QTL analysis, and mainly consisted of isolated markers. This is unlikely to
455 represent a case of multi-locus sex determination (Moore and Roberts 2013), as the evidence is
456 weak since there is little other corroborating information. The peaks on chromosomes 2, 3, and 5
457 consisted of solitary markers, while that on chromosome 1 included 5 markers that occurred
458 within a 1 kb interval. Our results are similar to those in *P. trichocarpa*, which also contained
459 multiple secondary GWAS peaks in a sex determination GWAS (Geraldès *et al.* 2015).
460 While some of the secondary *Populus* peaks appear to be assembly and/or alignment artifacts
461 (Geraldès *et al.* 2015), we found no evidence of assembly errors in these regions for *S. purpurea*
462 based on examining the sequence assembly itself as well as the underlying genetic map.
463 Problems with assembly of SDRs are common, presumably due to strong haplotype divergence
464 and high repeat composition, which impede assembly of short-read sequence data (Miller *et al.*
465 2010). Furthermore, the suppressed recombination in these regions inhibits map-based assembly
466 methods. An alternative explanation for the secondary peaks is recent translocation from those
467 chromosomes to the W chromosome in *S. purpurea*. If the W haplotype is not represented in the
468 reference genome assembly, then the reads derived from the recently-translocated regions could
469 align to their original locations. Short-read sequence aligners like Bowtie2 do not handle
470 repetitive sequences well, and commonly misalign reads derived from such regions (Lian *et al.*
471 2016).

472 The GWAS peak on chromosome 19 are especially interesting because it coincides with
473 the position of one of the SDRs in *Populus*. This peak also has more corroborating evidence than
474 the other secondary peaks because it had one of the lowest observed P-values, and it is
475 recapitulated in the QTL analysis. Furthermore, the peak on chromosome 3 best matches a
476 scaffold from the SDR region of *Populus* on chromosome 19, so at least two independent
477 association results point to sex-specific genotypes in genomic segments with homology to the
478 *Populus* SDR. If these represent recent translocations, then this could be a clue to the origin of
479 the chromosome 15 SDR in the *Salix* lineage.

480 **Recombination Suppression and Relative Age of the SDR**

481 Reduced recombination is a crucial component of sex chromosome evolution which
482 ensures that male and female sterility factors do not co-occur in the zygote (Bergero and
483 Charlesworth 2009; Ming *et al.* 2011). As expected, we observed reduced recombination across
484 most of the SDR in *S. purpurea* (Figure 5). This could be caused by large-scale structural
485 polymorphisms and reinforced by the accumulation of nonhomologous sequences in the female-
486 specific haplotype (Ming *et al.* 2011; Charlesworth 2015). The SDR also shows a higher
487 proportion of repetitive elements, as expected in regions with reduced recombination. Similar
488 features are also apparent within the SDR of *S. suchowensis* and *S. viminalis* (Hou *et al.* 2015;
489 Pucholt *et al.* 2015; Chen *et al.* 2016), but are not as apparent for the *P. trichocarpa* SDR, which
490 is estimated to be quite small (Gerald *et al.* 2015). If this is accurate, it could indicate that the
491 *P. trichocarpa* region has not yet developed these features, or that it is highly dynamic. In the
492 case of *S. purpurea*, the SDR is quite large, with a lower limit of 1.04 Mb (based on the
493 cumulative length of female-specific scaffolds), and an upper limit of approximately 5 Mb, based
494 on suppressed recombination and the occurrence of SNPs that are significantly associated with
495 sex. It is possible that the SDR overlaps with the centromere on chromosome 15, and this could
496 contribute to the large apparent size of the region of suppressed recombination. However, the
497 SDR does not contain any of the tandem minisatellite repeats that are apparently characteristic of
498 the *S. purpurea* centromeres, as identified in a previous study (Melters *et al.* 2013). It remains to
499 be seen if the lack of these repeats is due to poor assembly, or if the centromere is located
500 elsewhere on this chromosome.

501 Divergence between Z and W transcripts in the *S. purpurea* SDR is relatively low,
502 suggesting that suppression of recombination is incomplete or recently established. This is

503 similar to the SDRs of *P. trichocarpa* (Gerald *et al.* 2015) and *S. viminalis* (Pucholt, Wright, *et*
504 *al.* 2017), which also show low divergence of sex-specific sequences. Furthermore, we saw no
505 evidence of the presence of evolutionary strata within or around the *S. purpurea* SDR. Such
506 features occur due to the establishment of regions of suppressed recombination at different times
507 during sex chromosome evolution (Charlesworth 2016). Evolutionary strata are apparent in well-
508 established SDRs of other plants, including *Silene latifolia* (Bergero *et al.* 2007) and *Carica*
509 *papaya* (Wang *et al.* 2012). However, no such regions were detected in *S. suchowensis* (Pandey
510 and Azad 2016). Given the low divergence, lack of strata, and the frequent movement of the
511 SDR within the family, it is reasonable to conclude that the SDR is highly dynamic in this
512 family, and that sex determination loci frequently translocate to new positions and/or are
513 superseded by other loci on autosomes, as predicted by theoretical models of SDR movement
514 (van Doorn and Kirkpatrick 2007, 2010).

515

516 **Candidate Genes and Their Function**

517

518 The SDRs are genomic regions that are statistically associated with gender. This
519 association must be due to the presence of loci that control sex determination, but the regions
520 also likely harbor loci that are under sexually antagonistic selection (van Doorn and Kirkpatrick
521 2007; Bachtrog *et al.* 2014). The gene content of these regions could therefore provide insights
522 about mechanisms of sex determination as well as sex dimorphism. We identified 251 protein-
523 coding genes in the SDRs of *S. purpurea* (Table S8). Most have not been functionally annotated,
524 but clues can be inferred based on conserved domains and their predicted function in model
525 organisms. It is also important to note that the assembly problems mentioned previously have
526 probably prevented full enumeration of the gene content of the SDRs. This problem may be
527 particularly challenging for female-specific portions of the W chromosome (Pucholt *et al.* 2015).
528 Nevertheless, there are several genes in this region that could plausibly be involved in floral
529 development and sex-specific regulation that are worthy of consideration.

530 Since floral morphology is the most striking difference between the sexes, it is reasonable
531 to expect that genes involved in floral development would be located in the SDRs. Indeed, the
532 SDR contains SapurV1A.0718s0010, an ortholog of WUSCHEL-related homeotic genes (e.g.,
533 *WOX1*). Orthologs in other species, including STF in *Medicago truncatula*, LAM1 in *Nicotiana*
534 *sylvestris*, and MAW in *Petunia*, are key regulators of the lateral outgrowth of leaf blades and

535 floral organs (Lin *et al.* 2013). This gene showed slightly elevated expression in male shoot tips
536 compared to female shoot tips (Table S7).

537 Several genes in the SDR may be involved specifically with male development and
538 function. For example, our analysis of GO term over-representation highlighted the presence of
539 seven genes containing the kinesin motor domain (PF00225), which is involved in microtubule-
540 based movement or organelles, including during pollen tube growth (Cai and Cresti 2009). For
541 example, loss-of-function mutants of the closest homolog of SapurV1A.0530s0110 in
542 *Arabidopsis thaliana* (*NACK1*) showed reduced growth and prematurely-terminated petals,
543 pistils, and stamens (Nishihama *et al.* 2002).

544 Two other genes in the SDR may be related to pollen function. First,
545 SapurV1A.1741s0030, is a homolog of *PLANT INTRACELLULAR RAS GROUP-RELATED*
546 *LRR 3* (*PIRL3*), which has been implicated in pollen development in *Arabidopsis* (Forsthoefel *et*
547 *al.* 2013). The second, SapurV1A.0301s0130 is a homolog of the *Arabidopsis* gene
548 AT3G01570.1, a member of the oleosin family (Kim *et al.* 2002). This gene occurs in a female-
549 specific portion of the SDR and has female-biased gene expression, perhaps reflecting a potential
550 role in sex dimorphism in *Salix*. Other members of the oleosin family have been associated with
551 pollen wall development, and eight of these have been shown to have tapetal-specific expression
552 in *Arabidopsis* (Kim *et al.* 2002; Hsieh and Huang 2004; Yang *et al.* 2007). The expression of
553 one of these oleosin genes is regulated by *MALE STERILITY1* (*MS1*) in *Arabidopsis*, which
554 controls pollen and tapetal development (Yang *et al.* 2007), raising the possibility that altered
555 regulation of oleosin genes could provide a pathway to male sterility.

556 The SDR on chromosome 19 deserves special attention due to its shared homology with
557 the *Populus* SDR. One particularly interesting gene in this region is SapurV1A.1005s0060,
558 which contains a Small MutS-Related (SMR) domain and a domain of unknown function
559 (DUF1771). These domains frequently occur together in eukaryotes, but the function of
560 DUF1771 has yet to be characterized (Fukui and Kuramitsu 2011). Proteins with the SMR
561 domain, such as MutS2, can suppress (Fukui *et al.* 2007; Fukui and Kuramitsu 2011) or promote
562 (Burby and Simmons 2017) homologous recombination by endonucleolytic digestion, and are
563 involved in mismatch repair in diverse prokaryotes (Kunkel and Erie 2005). The roles of the
564 SMR domain in plants are not fully characterized, but when coupled with the pentatricopeptide
565 repeat motif, the SMR domain shows sequence-specific RNA endonuclease activity and affects

566 chloroplast function (Zhou *et al.* 2017). Due to its potential roles in recombination, mismatch
567 repair, and regulation of organellar function, this gene is an intriguing candidate in the context of
568 sex determination as well as mediation of the female-biased sex ratios that are commonly
569 observed in *Salix* (Alliende and Harper 1989; Alstrom-Rapaport *et al.* 1998; Ueno *et al.* 2007;
570 Pucholt, Hallingbäck, *et al.* 2017), including in *S. purpurea*, as reported here.

571 **Sex Chromosome Evolution in the Salicaceae**

572 *Populus* and *Salix* are closely-related genera that share many key characteristics, the most
573 notable of which is that they are both nearly fixed for dioecy. *Populus* first appears in the fossil
574 record between 40 and 60 MYA, apparently slightly earlier than *Salix* (Boucher *et al.* 2003).
575 However, *Populus* and *Salix* exhibit much less divergence in nucleotide sequence and
576 chromosome structure than expected, presumably due to long average generation times (Sterck *et*
577 *al.* 2005; Hou *et al.* 2016). It may therefore seem surprising that the chromosomal location and
578 gene content of the SDRs are so different, and that they have different heterogametic
579 configurations (Hou *et al.* 2015; Pucholt *et al.* 2015). In fact, movement of sex determination
580 loci and transitions between XY and ZW systems are well-known in organisms that lack
581 strongly-differentiated, heteromorphic sex chromosomes (Bachtrog *et al.* 2014).

582 A striking finding of this study is the existence of multiple sexually dimorphic regions in
583 the *S. purpurea* genome, one of which is on chromosome 15 and shared with other *Salix* species
584 (Pucholt *et al.* 2015; Chen *et al.* 2016), and one on chromosome 19, which harbors the SDR of
585 multiple *Populus* species (Tuskan *et al.* 2012; Kersten *et al.* 2014; Geraldès *et al.* 2015). There
586 are several lines of evidence to support a model whereby the original sex determination locus
587 was located on chromosome 19 in the common ancestor of *Salix* and *Populus*. First, *Salix*
588 chromosome 19 shows overall high synteny with *P. trichocarpa* chromosome 19, and both
589 species apparently have an SDR in the same region of this chromosome. In contrast,
590 chromosome 15 shows no sex chromosome characteristics in *Populus*, and the composition of
591 chromosome 15 is quite different in the *Salix* SDR. Second, we were unable to create a female
592 backcross map for *S. purpurea* chromosome 19, the only chromosome for which mapping failed.
593 This was due to a paucity of genetic markers in this region, particularly in the female backcross
594 configuration. Notably, such a configuration would be absent in the SDR of an XY sex
595 determination system. On the other hand, the overall lack of genetic markers is probably caused
596 in part by the high repeat content of this chromosome, which can inhibit genotyping based on

597 short read sequences (Treangen and Salzberg 2013). High repeat content is also expected in
598 regions of reduced recombination, commonly found in sex chromosomes (Ming and Moore
599 2007; Bergero and Charlesworth 2009). In summary, because chromosome 19 shows
600 characteristics of an SDR in *S. purpurea* and in multiple *Populus* species, but chromosome 15
601 only shows such characteristics in *Salix*, it is logical to hypothesize that chromosome 19 is the
602 ancestral sex chromosome in the Salicoid lineage.

603 In the present study, it is important to reemphasize that the locus mapped to chromosome
604 19 may be an assembly or alignment artifact. This could be caused by a recent translocation from
605 chromosome 19 to the W haplotype of chromosome 15, which would result in incorrect
606 alignment of GBS reads to the original chromosome 19 locus if the W haplotype is not in the
607 main genome assembly. However, because the locus matches a portion of the SDR of
608 chromosome 19 in *Populus*, and the gene content of these regions is similar between the taxa,
609 this finding would still provide valuable clues about sex determination and/or sex dimorphism in
610 this family even if it is caused by a recent translocation. It is also noteworthy that the *S. purpurea*
611 *de novo* genome assembly did not use the *P. trichocarpa* genome assembly as a reference to
612 guide placement of scaffolds in pseudomolecules (Smart et al., in preparation), so the results
613 reported here are not caused by carryover of biases or errors from the original *P. trichocarpa*
614 assembly.

615 Unfortunately, a definitive comparison of the Salicaceae sex chromosomes is not possible
616 with the currently-available genome sequences. The SDRs of *Salix* and *Populus* are typical in
617 that they have complex structural polymorphisms, high repeat content, and low recombination
618 rates, all of which contribute to fragmentary and erroneous genome assemblies (Geraldes *et al.*
619 2015). Efforts are underway to assemble these regions using long read sequencing and dense
620 genetic mapping in multiple pedigrees. This will facilitate analyses that can date the origin of
621 these regions based on differentiation of sex-specific haplotypes in the non-recombining portions
622 of the SDR (Otto *et al.* 2011). Furthermore, elucidation of the sex determination system in
623 additional Salicaceae taxa should help to determine the ancestral state. This family should
624 therefore be instrumental in advancing our knowledge of the evolution and ecological
625 significance of sex chromosomes as genetic and genomic resources continue to accumulate.

626 **Acknowledgements**

627

628 We are grateful to Matt Olson and two anonymous reviewers for helpful comments on
629 the manuscript. This work was supported by grants from the USDA-NIFA CAP program (4705-
630 WVU-USDA-9703), the DOE JGI Community Sequencing Program, and the NSF Dimensions
631 of Biodiversity Program (DEB-1542509). Sequencing was conducted by the U.S. Department of
632 Energy Joint Genome Institute, a DOE Office of Science User Facility, was supported by
633 the Office of Science of the U.S. Department of Energy under Contract No. DE-AC02-
634 05CH11231.

635 **Supplementary Materials**

636

637 **Figure S1** Pairwise Scaled Identity by State (IBS) for the (a) complete association population
638 (N=112), (b) the complete F₂ full sib Family (N=497), and (c) the association population with
639 clones removed (N=75). The IBS cutoff used for identifying clonal pairs was 0.9.

640 **Figure S2** Frequency of mapped markers with and without segregation distortion in family 317
641 for males and females. A. Markers in female-backcross configuration. B. Markers in male-
642 backcross configuration. Notice the lack of undistorted (normal) markers on chromosome 19 in
643 female backcross configuration.

644 **Figure S3** Quantile–Quantile (Q–Q) plots of observed and expected P-values for the GWAS for
645 sex. Red line indicates $X = Y$.

646 **Figure S4** Stacked histogram of average observed heterozygosity for males, females, and
647 hermaphrodites for sex-associated loci in the *S. purpurea* association population.

648 **Figure S5** Distribution of differences in null allele frequency between females and males in the
649 association population. Extreme values are shaded in red.

650 **Figure S6** Proportion of reference sequence gaps (“assembly Ns”) in regions that showed no
651 coverage in the female (a) or male (b) reference-based alignments. The male had 0 coverage
652 primarily in regions with minimal reference gaps, suggesting that these are regions that are
653 present in the female sequence and absent in the male.

654 **Figure S7** Box plot showing that the proportion of repeat elements is elevated in the SDR.

655 **Figure S8** Dot plot derived from aligning the *S. suchowensis* SDR (primarily located on
656 scaffold64) to *S. purpurea* chromosome 15 using lastz.

657 **Figure S9** Alignment of Kinesin genes from the SDR of *S. purpurea* and their closest ortholog in
658 *P. trichocarpa*. SapurV1A.1267s0010 is artificially truncated due to an assembly gap
659 overlapping with the gene. Conserved domains are highlighted and labeled. Tandem duplicate
660 pairs are 1.) SapurV1A.0719s0080 and SapurV1A.0719s0090; and 2.) SapurV1A.1267s0010 and
661 SapurV1A.1267s0020.

662

663 **Table S1** Significant markers (LOD>3.5) from QTL mapping of sex. The table includes linkage
664 group (LG), map positions (in centimorgans), map type (female backcross, F, male backcross,
665 M, and intercross, IC), the physical scaffold from the genome assembly, the physical position of
666 the marker in the genome assembly, and the frequency of different genotype configurations in
667 the progeny.

668 **Table S2** Number of unfiltered GBS markers produced by the Tassel pipeline for the F₂ family
669 317. Markers/100kb is the average number of markers per 100 kb interval. F:M Backcross is the
670 ratio of markers in a Female Backcross configuration (heterozygous in the female parent,
671 homozygous in the male parent) to markers in the Male Backcross configuration (homozygous in
672 female parent, heterozygous in male parent).

673 **Table S3** Results of GWAS for sex. The table includes all significant markers ($p < 1 \times 10^{-7}$).

674 **Table S4** Best matches for secondary *S. purpurea* SDRs to the *S. purpurea* and *P. trichocarpa*
675 genomes. “Secondary Blast Hit” is the best blastn hit to the *S. purpurea* genome, after excluding
676 self hits.

677 **Table S5** Markers showing a female-specific genotype configuration (one allele observed in
678 females, none in males). These are presumably derived from W segments included in the genome
679 assembly.

680 **Table S6** Scaffolds with >30% female-specific sequence. “Proportion W” is a calculation based
681 on the proportion of the scaffold, after excluding gaps, that is present in the female sequence but
682 absent in the male sequence (Female-Specific).

683 **Table S7** Repeat composition of the *S. purpurea* chromosomes.

684 **Table S8** Predicted genes found within the SDR of *S. purpurea*. “W Overlap” and “W
685 proportion” represent the intersection of the location of the gene with female-specific genome
686 segments. Omega values are the ratio of nonsynonymous (dN) to synonymous (dS) substitutions

687 between the *S. purpurea* and *P. trichocarpa* orthologs. Multiple values are provided in cases
688 with multiple *Populus* orthologs, presumably due to lineage-specific expansion.

689

690 Literature Cited

691

692 Ainsworth, C., 2000 Boys and girls come out to play: The molecular biology of dioecious plants.
693 Ann. Bot. 86: 211–221.

694 Alliende, M. C., and J. L. Harper, 1989 Demographic studies of a dioecious tree. I. Colonization,
695 sex and age structure of a population of *Salix cinerea*. J. Ecol. 77: 1029–1047.

696 Alstrom-Rapaport, C., M. Lascoux, Y. C. Wang, G. Roberts, and G. A. Tuskan, 1998
697 Identification of a RAPD marker linked to sex determination in the basket willow (*Salix*
698 *viminalis* L.). J. Hered. 89: 44–49.

699 Andrews, K. R., J. M. Good, M. R. Miller, G. Luikart, and P. A. Hohenlohe, 2016 Harnessing
700 the power of RADseq for ecological and evolutionary genomics. Nat Rev Genet 17: 81–92.

701 Arends, D., P. Prins, R. C. Jansen, and K. W. Broman, 2010 R/qtl: High-throughput multiple
702 QTL mapping. Bioinformatics 26: 2990–2992.

703 Argus, G. W., 1997 Infrageneric classification of *Salix* (Salicaceae) in the new world. Syst. Bot.
704 Monogr. 52: 1–121.

705 Ashman, T.-L., 2006 The evolution of separate sexes: a focus on the ecological context, pp. 370
706 in *Ecology and evolution of flowers*, edited by L. D. Harder and S. C. H. Barrett. Oxford
707 University Press, Oxford.

708 Ashman, T.-L., A. Kwok, and B. C. Husband, 2013 Revisiting the Dioecy-Polyploidy
709 Association: Alternate Pathways and Research Opportunities. Cytogenet. Genome Res. 140:
710 241–255.

711 Bachtrog, D., J. Mank, C. L. Peichel, M. Kirkpatrick, S. P. Otto *et al.*, 2014 Sex Determination:
712 Why So Many Ways of Doing It? PLoS Biol. 12: e1001899.

713 Barrett, S. C. H., and J. Hough, 2013 Sexual dimorphism in flowering plants. J. Exp. Bot. 64:
714 67–82.

715 Bergero, R., and D. Charlesworth, 2009 The evolution of restricted recombination in sex
716 chromosomes. *Trends Ecol. Evol.* 24: 94–102.

717 Bergero, R., A. Forrest, E. Kamau, and D. Charlesworth, 2007 Evolutionary strata on the X
718 chromosomes of the dioecious plant *Silene latifolia*: Evidence from new sex-linked genes.
719 *Genetics* 175: 1945–1954.

720 Boucher, L. D., S. R. Manchester, and W. S. Judd, 2003 An extinct genus of Salicaceae based on
721 twigs with attached flowers, fruits, and foliage from the Eocene Green River Formation of
722 Utah and Colorado, USA. *Am. J. Bot.* 90: 1389–1399.

723 Burby, P. E., and L. A. Simmons, 2017 MutS2 promotes homologous recombination in *Bacillus*
724 *subtilis*. *J. Bacteriol.* 199: e00682-16.

725 Cai, G., and M. Cresti, 2009 Organelle motility in the pollen tube: a tale of 20 years. *J. Exp. Bot.*
726 60: 495–508.

727 Carlson, C. H., Y. Choi, A. P. Chan, M. J. Serapiglia, C. D. Town *et al.*, 2017 Dominance and
728 Sexual Dimorphism Pervade the *Salix purpurea* L. Transcriptome. *Genome Biol. Evol.* 9:
729 2377–2394.

730 Charlesworth, D., 2006 Evolution of Plant Breeding Systems. *Curr. Biol.* 16: 726–735.

731 Charlesworth, D., 2015 Plant contributions to our understanding of sex chromosome evolution.
732 *New Phytol.* 208: 52–65.

733 Charlesworth, D., 2016 Plant Sex Chromosomes. *Annu. Rev. Plant Biol.* 67: 397–420.

734 Charlesworth, D., and B. Charlesworth, 1978 Population genetics of partial male-sterility and the
735 evolution of monoecy and dioecy. *Heredity* 41: 137–153.

736 Charnov, E. L., 1982 The theory of sex allocation. *Monogr. Popul. Biol.* 18: 1–355.

737 Chen, Y., T. Wang, L. Fang, X. Li, and T. Yin, 2016 Confirmation of single-locus sex
738 determination and female heterogamety in willow based on linkage analysis. *PLoS One* 11:
739 e0147671.

740 DePristo, M. a, E. Banks, R. Poplin, K. V Garimella, J. R. Maguire *et al.*, 2011 A framework for
741 variation discovery and genotyping using next-generation DNA sequencing data. *Nat.*
742 *Genet.* 43: 491–8.

743 Dickmann, D. I., and J. Kuzovkina, 2014 Poplars and willows of the world, with emphasis on
744 silviculturally important species., pp. 8–91 in *Poplars and willows: trees for society and the*
745 *environment*, CABI, Wallingford.

746 van Doorn, G. S., and M. Kirkpatrick, 2010 Transitions between male and female heterogamety
747 caused by sex-antagonistic selection. *Genetics* 186: 629–645.

748 van Doorn, G. S., and M. Kirkpatrick, 2007 Turnover of sex chromosomes induced by sexual
749 conflict. *Nature* 449: 909–912.

750 Elshire, R. J., J. C. Glaubitz, Q. Sun, J. a. Poland, K. Kawamoto *et al.*, 2011 A robust, simple
751 genotyping-by-sequencing (GBS) approach for high diversity species. *PLoS One* 6: e19379.

752 Falda, M., S. Toppo, A. Pescarolo, E. Lavezzo, B. Di Camillo *et al.*, 2012 Argot2: a large scale
753 function prediction tool relying on semantic similarity of weighted Gene Ontology terms.
754 *BMC Bioinformatics* 13: S14.

755 Forsthoefel, N., K. Klag, B. Simeles, R. Reiter, L. Brougham *et al.*, 2013 The *Arabidopsis* Plant
756 Intracellular Ras-group LRR (PIRL) Family and the Value of Reverse Genetic Analysis for
757 Identifying Genes that Function in Gametophyte Development. *Plants* 2: 507–520.

758 Fukui, K., H. Kosaka, S. Kuramitsu, and R. Masui, 2007 Nuclease activity of the MutS
759 homologue MutS2 from *Thermus thermophilus* is confined to the Smr domain. *Nucleic*
760 *Acids Res.* 35: 850–860.

761 Fukui, K., and S. Kuramitsu, 2011 Structure and Function of the Small MutS-Related Domain.
762 *Mol. Biol. Int.* 2011: 1–9.

763 Füssel, U., S. Dötterl, A. Jürgens, and G. Aas, 2007 Inter- and Intraspecific Variation in Floral
764 Scent in the Genus *Salix* and its Implication for Pollination. *J. Chem. Ecol.* 33: 749–765.

765 Gaudet, M., V. Jorge, I. Paolucci, I. Beritognolo, G. S. Mugnozza *et al.*, 2008 Genetic linkage
766 maps of *Populus nigra* L. including AFLPs, SSRs, SNPs, and sex trait. *Tree Genet.*
767 *Genomes* 4: 25–36.

768 Geraldès, A., C. A. Hefer, A. Capron, N. Kolosova, F. Martínez-Nuñez *et al.*, 2015 Recent Y
769 chromosome divergence despite ancient origin of dioecy in poplars (*Populus*). *Mol. Ecol.*
770 24: 3243–3256.

771 Glaubitz, J. C., T. M. Casstevens, F. Lu, J. Harriman, R. J. Elshire *et al.*, 2014 TASSEL-GBS: A
772 high capacity genotyping by sequencing analysis pipeline. PLoS One 9: e0090346.

773 Glick, L., N. Sabath, T. L. Ashman, E. Goldberg, and I. Mayrose, 2016 Polyploidy and sexual
774 system in angiosperms: Is there an association? Am. J. Bot. 103: 1223–1235.

775 Gnerre, S., I. MacCallum, D. Przybylski, F. J. Ribeiro, J. N. Burton *et al.*, 2011 High-quality
776 draft assemblies of mammalian genomes from massively parallel sequence data. Proc. Natl.
777 Acad. Sci. U. S. A. 108: 1513–1518.

778 Goodstein, D. M., S. Shu, R. Howson, R. Neupane, R. D. Hayes *et al.*, 2012 Phytozome: a
779 comparative platform for green plant genomics. Nucleic Acids Res. 40: D1178–D1186.

780 Hou, J., N. Ye, Z. Dong, M. Lu, L. Li *et al.*, 2016 Major chromosomal rearrangements
781 distinguish willow and poplar after the ancestral “Salicoid” genome duplication. Genome
782 Biol. Evol. 8: 1868–1875.

783 Hou, J., N. Ye, D. Zhang, Y. Chen, L. Fang *et al.*, 2015 Different autosomes evolved into sex
784 chromosomes in the sister genera of *Salix* and *Populus*. Sci. Rep. 5: e9076.

785 Hsieh, K., and A. H. C. Huang, 2004 Endoplasmic reticulum, oleosins, and oils in seeds and
786 tapetum cells. Plant Physiol. 136: 3427–3434.

787 Kang, H. M., J. H. Sul, S. K. Service, N. a Zaitlen, S.-Y. Kong *et al.*, 2010 Variance component
788 model to account for sample structure in genome-wide association studies. Nat. Genet. 42:
789 348–354.

790 Karp, A., S. J. Hanley, S. O. Trybush, W. Macalpine, M. Pei *et al.*, 2011 Genetic Improvement
791 of Willow for Bioenergy and Biofuels. J. Integr. Plant Biol. 53: 151–165.

792 Karrenberg, S., J. Kollmann, and P. J. Edwards, 2002 Pollen vectors and inflorescence
793 morphology in four species of *Salix*. Plant Syst. Evol. 235: 181–188.

794 Kersten, B., B. Pakull, K. Groppe, J. Lueneburg, and M. Fladung, 2014 The sex-linked region in
795 *Populus tremuloides* Turesson 141 corresponds to a pericentromeric region of about two
796 million base pairs on *P. trichocarpa* chromosome 19. Plant Biol. 16: 411–418.

797 Kim, H. U., K. Hsieh, C. Ratnayake, and A. H. C. Huang, 2002 A novel group of oleosins is
798 present inside the pollen of *Arabidopsis*. J. Biol. Chem. 277: 22677–22684.

799 Kunkel, T. a, and D. a Erie, 2005 DNA mismatch repair. *Annu. Rev. Biochem.* 74: 681–710.

800 Lian, S., T. Liu, K. Gong, X. Chen, and G. Zheng, 2016 A Complete and Accurate Short
801 Sequence Alignment Algorithm for Repeats. *J. Biosci. Med.* 4: 144–151.

802 Lin, H., L. Niu, N. a McHale, M. Ohme-Takagi, K. S. Mysore *et al.*, 2013 Evolutionarily
803 conserved repressive activity of WOX proteins mediates leaf blade outgrowth and floral
804 organ development in plants. *Proc. Natl. Acad. Sci. U. S. A.* 110: 366–371.

805 Lloyd, D. G., 1979 Evolution towards dioecy in heterostylous populations. *Plant Syst. Evol.* 131:
806 71–80.

807 Mank, J. E., 2009 Sex chromosomes and the evolution of sexual dimorphism: lessons from the
808 genome. *Am. Nat.* 173: 141–150.

809 Melters, D. P., K. R. Bradnam, H. a Young, N. Telis, M. R. May *et al.*, 2013 Comparative
810 analysis of tandem repeats from hundreds of species reveals unique insights into centromere
811 evolution. *Genome Biol.* 14: R10.

812 Miller, J. R., S. Koren, and G. Sutton, 2010 Assembly algorithms for next-generation sequencing
813 data. *Genomics* 95: 315–27.

814 Ming, R., A. Bendahmane, and S. S. Renner, 2011 Sex chromosomes in land plants. *Annu. Rev.*
815 *Plant Biol.* 62: 485–514.

816 Ming, R., and P. H. Moore, 2007 Genomics of sex chromosomes. *Curr. Opin. Plant Biol.* 10:
817 123–130.

818 Mock, K. E., C. M. Callahan, M. N. Islam-Faridi, J. D. Shaw, H. S. Rai *et al.*, 2012 Widespread
819 triploidy in western North American aspen (*Populus tremuloides*). *PLoS One* 7: e48406.

820 Moore, E. C., and R. B. Roberts, 2013 Polygenic sex determination. *Curr. Biol.* 23: R510-2.

821 Nicolas, M., G. Marais, V. Hykelova, B. Janousek, V. Laporte *et al.*, 2005 A gradual process of
822 recombination restriction in the evolutionary history of the sex chromosomes in dioecious
823 plants. *PLoS Biol.* 3: e4.

824 Nishihama, R., T. Soyano, M. Ishikawa, S. Araki, H. Tanaka *et al.*, 2002 Expansion of the cell
825 plate in plant cytokinesis requires a kinesin-like protein/MAPKKK complex. *Cell* 109: 87–
826 99.

827 Olson, M. S., J. L. Hamrick, and R. C. Moore, 2017 Breeding systems, mating systems, and
828 gender determination in angiosperm trees, in *Comparative and Evolutionary Genomics of*
829 *Angiosperm Trees*, edited by A. Groover and Q. C. B. Cronk. Springer International
830 Publishing, Switzerland.

831 Otto, S. P., J. R. Pannell, C. L. Peichel, T.-L. Ashman, D. Charlesworth *et al.*, 2011 About PAR:
832 the distinct evolutionary dynamics of the pseudoautosomal region. *Trends Genet.* 27: 358–
833 367.

834 Pakull, B., K. Groppe, M. Meyer, T. Markussen, and M. Fladung, 2009 Genetic linkage mapping
835 in aspen (*Populus tremula* L. and *Populus tremuloides* Michx.). *Tree Genet. Genomes* 5:
836 505–515.

837 Pakull, B., B. Kersten, J. Lüneburg, and M. Fladung, 2014 A simple PCR-based marker to
838 determine sex in aspen. *Plant Biol.* 17: 256–261.

839 Pandey, R. S., and R. K. Azad, 2016 Deciphering evolutionary strata on plant sex chromosomes
840 and fungal mating-type chromosomes through compositional segmentation. *Plant Mol. Biol.*
841 90: 359–373.

842 Paolucci, I., M. Gaudet, V. Jorge, I. Beritognolo, S. Terzoli *et al.*, 2010 Genetic linkage maps of
843 *Populus alba* L. and comparative mapping analysis of sex determination across *Populus*
844 species. *Tree Genet. Genomes* 6: 863–875.

845 Peto, F. H., 1938 Cytology of poplar species and natural hybrids. *Can. J. Res.* 16: 446–455.

846 Price, A. L., N. J. Patterson, R. M. Plenge, M. E. Weinblatt, N. a Shadick *et al.*, 2006 Principal
847 components analysis corrects for stratification in genome-wide association studies. *Nat.*
848 *Genet.* 38: 904–909.

849 Pucholt, P., H. R. Hallingbäck, and S. Berlin, 2017 Allelic incompatibility can explain female
850 biased sex ratios in dioecious plants. *BMC Genomics* 18: 251.

851 Pucholt, P., A.-C. Rönnberg-Wästljung, and S. Berlin, 2015 Single locus sex determination and
852 female heterogamety in the basket willow (*Salix viminalis* L.). *Heredity* 114: 575–583.

853 Pucholt, P., A. E. Wright, L. L. Conze, J. E. Mank, and S. Berlin, 2017 Recent Sex Chromosome
854 Divergence despite Ancient Dioecy in the Willow, *Salix viminalis*. *Mol. Biol. Evol.* 22:

855 522–525.

856 Renner, S. S., 2014 The relative and absolute frequencies of angiosperm sexual systems: dioecy,
857 monoecy, gynodioecy, and an updated online database. *Am. J. Bot.* 101: 1588–1596.

858 Rice, W. W. R., 1984 Sex chromosomes and the evolution of sexual dimorphism. *Evolution* 38:
859 1416–1424.

860 Serapiglia, M. J., F. E. Gouker, J. F. Hart, F. Unda, S. D. Mansfield *et al.*, 2015 Ploidy Level
861 Affects Important Biomass Traits of Novel Shrub Willow (*Salix*) Hybrids. *BioEnergy Res.*
862 8: 259–269.

863 Slavov, G. T., and P. Zhelev, 2010 Salient Biological Features, Systematics, and Genetic
864 Variation of *Populus*, pp. 15–38 in *Genetics and Genomics of Populus*, edited by S.
865 Jansson, R. P. Bhalerao, and A. Groover. Springer New York, New York, NY.

866 Sterck, L., S. Rombauts, S. Jansson, F. Sterky, P. Rouzé *et al.*, 2005 EST data suggest that poplar
867 is an ancient polyploid. *New Phytol.* 167: 165–170.

868 Temmel, N. A., H. S. Rai, and Q. C. B. Cronk, 2007 Sequence characterization of the putatively
869 sex-linked Ssu72 -like locus in willow and its homologue in poplar. *Can. J. Bot.* 85: 1092–
870 1097.

871 Treangen, T. J., and S. L. Salzberg, 2013 Repetitive DNA and next-generation sequencing:
872 computational challenges and solutions. *Nat Rev Genet.* 13: 36–46.

873 Tuskan, G. A., S. DiFazio, P. Faivre-Rampant, M. Gaudet, A. Harfouche *et al.*, 2012 The
874 obscure events contributing to the evolution of an incipient sex chromosome in *Populus*: a
875 retrospective working hypothesis. *Tree Genet. Genomes* 8: 559–571.

876 Tuskan, G. A., S. DiFazio, S. Jansson, J. Bohlmann, I. Grigoriev *et al.*, 2006 The genome of
877 black cottonwood, *Populus trichocarpa* (Torr. & Gray). *Science* 313: 1596–1604.

878 Ueno, N., Y. Suyama, and K. Seiwa, 2007 What makes the sex ratio female-biased in the
879 dioecious tree *Salix sachalinensis*? *J. Ecol.* 95: 951–959.

880 Vyskot, B., and R. Hobza, 2015 The genomics of plant sex chromosomes. *Plant Sci.* 236: 126–
881 135.

882 Wang, J., J. Na, Q. Yu, A. R. Gschwend, J. Han *et al.*, 2012 Sequencing papaya X and Y h

883 chromosomes reveals molecular basis of incipient sex chromosome evolution. Proc. Natl.
884 Acad. Sci. 109: 13710–13715.

885 Yang, Z., 2007 PAML 4: phylogenetic analysis by maximum likelihood. Mol. Biol. Evol. 24:
886 1586–1591.

887 Yang, C., G. Vizcay-Barrena, K. Conner, and Z. a Wilson, 2007 MALE STERILITY1 is
888 required for tapetal development and pollen wall biosynthesis. Plant Cell 19: 3530–3548.

889 Yin, T., S. P. DiFazio, L. E. Gunter, X. Zhang, M. M. Sewell *et al.*, 2008 Genome structure and
890 emerging evidence of an incipient sex chromosome in *Populus*. Genome Res. 18: 422–430.

891 Zhou, W., Q. Lu, Q. Li, L. Wang, S. Ding *et al.*, 2017 PPR-SMR protein SOT1 has RNA
892 endonuclease activity. Proc. Natl. Acad. Sci. U. S. A. 114: E1554–E1563.

893